



Published in final edited form as:

*Biol Psychiatry*. 2016 December 01; 80(11): 836–848. doi:10.1016/j.biopsych.2015.12.012.

## Ablation of Type III Adenylyl Cyclase in Mice Causes Reduced Neuronal Activity, Altered Sleep Pattern, and Depression-Like Phenotypes

Xuanmao Chen<sup>1,\*</sup>, Jie Luo<sup>1,4</sup>, Yihua Leng<sup>1</sup>, Yimei Yang<sup>1</sup>, Larry S. Zweifel<sup>1,2</sup>, Richard D. Palmiter<sup>3</sup>, and Daniel R. Storm<sup>1</sup>

<sup>1</sup>Department of Pharmacology, School of Medicine, University of Washington, Seattle, WA 98195, USA

<sup>2</sup>Department of Psychiatry and Behavioral Sciences, School of Medicine, University of Washington, Seattle, WA 98195, USA

<sup>3</sup>Howard Hughes Medical Institute, Department of Biochemistry, School of Medicine, University of Washington, Seattle, WA 98195, USA

### Abstract

**Background**—Although major depressive disorder (MDD) has low heritability, a genome-wide association study in humans has recently implicated type 3 adenylyl cyclase (AC3, *ADCY3*) in MDD. Moreover, the expression level of AC3 in blood has been considered as a MDD biomarker in humans, but there is lack of supporting evidence from animal study.

**Methods**—We employed multiple approaches to experimentally evaluate if AC3 is a contributing factor for major depression using mouse models lacking *Adcy3* gene.

**Results**—We found that conventional AC3 KO mice exhibited phenotypes associated with MDD in behavioral assays. Electroencephalography/electromyography (EEG/EMG) recordings indicated that AC3 KO mice also have altered sleep patterns characterized by increased percentage of REM sleep. Sholl analysis revealed that cultured cortical neurons from AC3 KO mice have reduced dendritic arborization. Furthermore, synaptic activity at CA3-CA1 synapses was significantly lower in KO mice and they also exhibited attenuated long-term potentiation as well as deficits in spatial navigation. To confirm that these defects are not secondary responses to anosmia or developmental defects, we generated a conditional AC3 floxed mouse strain. This enabled us to inactivate AC3 function selectively in the forebrain and to inducibly ablate it in adult mice. Both

\*Correspondence should be addressed to: Dr. Xuanmao Chen, Department of Pharmacology, Mail Box 357280, Health Sciences Building, University of Washington, Seattle, Washington 98195-7750, Telephone 206-543-9280, Fax: 206-616-8621, chenx8@u.washington.edu.

<sup>4</sup>Present address: College of Life Sciences, Wuhan University, Wuhan, Hubei, China

**Financial Disclosures:** the authors declare no conflict of interests associated with this manuscript.

### Author's contribution

X.C. and D.R.S. conceived and designed experiments. X.C. performed experiments and data analysis. J.L. determined the hippocampal size and Y.L. performed Sholl analysis of cultured neurons. X.C., Y.L., Y.Y. and R.D.P. generated AC3 floxed mice and bred conditional AC3 knockout mice. L.S.Z. and R.D.P. provided experimental support and research agents. X.C. and D.R.S. wrote the paper.

AC3 forebrain-specific and AC3 inducible knockout mice exhibited pro-depression phenotypes without anosmia.

**Conclusion**—This study demonstrates that loss of AC3 in mice leads to decreased neuronal activity, altered sleep pattern, and depression-like behaviors, providing strong evidence supporting AC3 as a candidate gene for MDD.

---

## INTRODUCTION

MDD affects approximately 17 percent of the US population and is one of the most common debilitating disorders with lifetime prevalence of ~15% [1]. MDD has a complex and heterogeneous nature and is considered to be the outcome of gene–environmental interactions [1, 2]. Studies using mouse models have suggested that depression may result from loss of synapses and correspondingly altered neuronal activity in limbic and cortical regions [3–6]. Consequently, the limbic-cortical system is considered to be one of important regions implicated in the etiology and treatment of depression [3–5]. Current pharmacological treatments of depression rely on elevating monoamine concentrations in the brain [4]. Interestingly, most antidepressants, including selective serotonin re-uptake inhibitors have the potential to indirectly stimulate adenylyl cyclase activity through G-protein coupled adrenergic and serotonin receptors. Indeed, a number of studies have implicated adenylyl cyclase activity in depression [7] and platelet adenylyl cyclase activity has been proposed as a biological marker for MDD [8, 9]. This is based on the fact that subjects with a history of depression have lower mean levels of platelet adenylyl cyclase activity compared to control subjects. The major adenylyl cyclase in platelets is AC3 [10]. AC3 is also the predominant adenylyl cyclase in primary cilia throughout the central nervous system (CNS) [11, 12]. It is widely accepted that primary cilia are the cellular antenna for most of vertebrate cells including central neurons. Neuronal primary cilia do not have synaptic structure and largely depend on metabotropic receptors and downstream signal proteins to execute their functions. In this sense, AC3 is a key mediator of the cAMP signaling in primary cilia of the brain.

MDD is familial but has low heritability compared to other major psychiatric disorders [1, 4, 5, 13]. However, a recent study based on thousands of patients with MDD and healthy subjects has implicated cAMP signaling in depression and identified AC3 (*ADCY3*) as a top ranked gene relevant for MDD [14]. Consistently, depressed patients have decreased transcript levels of AC3 in blood [15]. Therefore, we examined the role of AC3 in depression using transgenic mice lacking AC3. We found that conventional AC3 KO mice exhibited depression-like behaviors. Moreover, we also generated a floxed AC3 mouse strain that allowed us to specifically ablate AC3 in a temporal- and tissue-dependent manner. Experimental evidence from conditional knockout mice also support AC3 as a gene associated with depression.

## METHODS AND Materials

Supplemental Information includes detailed Methods and Materials.

## Mice

AC3 KO mice and AC3 WT littermates were bred from heterozygotes and genotyped as previously reported [16, 17]. The mice used in behavioral analysis were age-matched 2.5 to 4 month-old males with comparable body weight, if not otherwise indicated. Mice were maintained on a 12-h light/dark cycle at 22°C and had access to food and water *ad libitum*.

## EEG/EMG headmount implantations, signal recordings and data analysis

Each mouse (3 to 4 months old, male) was implanted with an EEG/EMG headmount following the manufacturer's instructions (Pinnacle Technology, Lawrence, Kansas).

## Volume measurement of hippocampal regions

Volume estimation of CA1 and DG subregion was conducted using the Cavalieri Estimator probe of Stereo Investigator software (MBF Bioscience) on a Zeiss Axio Imager with a ×5 objective (NA 0.16). The volume of each subregion was determined by multiplying the total grid points for per subregion by the section thickness.

## Sholl analyses of morphology of primarily cultured cortical neurons from AC3 WT or KO mice

Sholl analyses of neuronal morphology were performed as previously described with some modifications [18]. Cortical neurons were isolated and cultured from AC3 WT or AC3 KO newborn pups at postnatal day 1, as previously described [19].

## Local field potential recording in acute brain slices

Local field recording was performed as previously described [20].

## Whole cell blind-patch recording of pyramidal neurons in CA1 region

Hippocampal slices were cut from young AC3 WT and AC3 KO mice (4–6 weeks) under ice-cold high magnesium sucrose solution: 87 mM NaCl, 2.5 mM KCl, 7 mM MgCl<sub>2</sub>, 0.5 mM CaCl<sub>2</sub>, 1.25 mM NaH<sub>2</sub>PO<sub>4</sub>, 25 mM NaHCO<sub>3</sub>, 10 mM D-glucose and 75 mM sucrose. After cutting, slices were placed in aCSF to recover for 1–2 hours at room temperature. Whole-cell mode was achieved using the “blind” patch method [21].

## Fiber fluorescence confocal endomicroscopy calcium imaging

We used FFE, an advanced *in vivo* calcium imaging system (Cellvizio Neuropak™ deep brain imaging system, Mauna Kea Technologies) in combination with viral-mediated gene delivery to hippocampal CA1 region to monitor overall CA1 neuronal activation in response to stimulation [22–24].

## Electroolfactogram (EOG) Recording

EOG recording were performed as previously described [17].

## Data analysis

Data were analyzed with GraphPad Prism 5 or with Clampfit 10.0 software (Axon Instruments), using Student's t-test, one-way ANOVA with Tukey post hoc test and two-way

ANOVA with Bonferroni's post hoc comparison or using Kolmogorov-Smirnov test to compare samples with probability distributions, If not specifically indicated in the Figure Legend; statistical analysis was unpaired student t-test with a two-tailed distribution. n.s. not significant, \*  $p < .05$ , \*\*  $p < .01$ , \*\*\*  $p < .001$ . Data was considered as statistically significant if  $p$  value  $< .05$  and values in the graph are expressed

## RESULTS

### AC3 KO mice Demonstrate Depression-like Behaviors

AC3 KO mice were subjected to a number of behavioral assays for depression including the tail suspension test, forced swim test, sociability test, novelty-suppressed feeding and nesting behavior. In the tail-suspension test, AC3 KO mice demonstrated significantly longer periods of immobility than their AC3 WT littermates (Fig 1A). Similarly, AC3 KO mice exhibited longer periods of immobility in the forced swim test than AC3 WT mice (Fig 1B). Furthermore, AC3 KO mice spent much less time interacting with a target mouse compared to AC3 WT mice in a 3-chamber sociability test (Fig 1C). When feeding in a novel environment, AC3 KO mice were much slower to feed than AC3 WT mice (Fig 1D) and their total feeding time in a novel environment was much less than AC3 WT mice (Fig 1E). When examined for drinking behavior in a novel environment, AC3 KO mice were slower to begin drinking (Fig 1F) and their total drinking time was markedly reduced (Fig 1G). AC3 KO mice also had lower coat score compared to AC3 WT mice, another marker for depression. Moreover, AC3 KO mice also exhibited defects in nesting behavior. Although they prepared nests in their home cages, their nests were poorly constructed compared to AC3 WT mice (Fig 1H and I). When placed in a novel environment, which posed mild stress to mice, the nest-building behavior of AC3 KO mice compared to AC3 WT mice was more impaired (Fig 1J and K). Collectively, these data indicate that AC3 KO mice exhibit behaviors consistent with depression.

### AC3 KO mice Spend More Time in Rapid Eye Movement (REM) Sleep

Disturbances of sleep including alterations in sleep architecture and increased REM sleep are typical for MDD patients and are one of the core symptoms associated with MDD [25, 26]. Therefore, the sleep architecture of AC3 KO mice was analyzed by EEG/EMG recordings. During a 24-h period, AC3 KO mice spent approximately the same amount of time awake as AC3 WT mice (Fig 2A and 2B). However, AC3 KO mice spent significantly more time than AC3 WT mice in REM sleep during the 24-hr light/dark period (Fig 2A and 2C). Throughout the circadian cycle, AC3 KO mice spent approximately twice as much the time in REM sleep as AC3 WT mice (Fig 2C). Moreover, AC3 KO mice demonstrated altered non-rapid eye movement (NREM) sleep patterns compared to WT littermates (Fig 2D). In addition, The NREM sleep wave was less synchronized in AC3 KO mice (Fig 2E and 2F). EEG power analysis of NREM sleep wave revealed that the peak power (power at peak frequency) and the total delta power (0.5–4Hz) of NREM sleep wave of AC3 KO mice were markedly reduced compared to AC3 WT mice (Fig 2F to 2H). These data indicate that AC3 KO mice have altered sleep pattern and sleep less efficiently than AC3 WT mice.

### Loss of AC3 Causes Neuronal Atrophy

Major depression is associated with neuronal atrophy in the CNS which is centered in the hippocampus [6]. We thereby examined if the hippocampal volume of AC3 KO mice is decreased. Indeed, AC3 KO mice have smaller hippocampi than their littermate controls (Fig 3A). Stereological analysis of AC3 KO brain sections further revealed that both area CA1 (Fig 3B) and the dentate gyrus (Fig 3C) of the hippocampus are significantly smaller than wild-type littermates. These data indicate that AC3 KO mice have reduced volume of hippocampi than their WT littermates.

AC3 is found in primary cilia in pyramidal neurons of the hippocampus and is implicated in dendritic arborization [18]. Therefore, we compared the morphology of primarily cultured cortical neurons from AC3 KO mice with those from AC3 WT mice (Fig 3D). Sholl analysis demonstrated that cultured cortical neurons from AC3 KO mice have reduced dendritic arborization compared to those from AC3 WT mice (Fig 3E), in line with previous data suggesting that AC3 regulates dendritic arborization of neurons [18]. These data indicate that AC3 in neuronal primary cilia regulates the morphology of neuronal dendrites, suggesting that loss of AC3 leads to neuronal atrophy.

### Synaptic Activity at the CA3-CA1 Schaffer-Collateral Synapse and CA1 Neuronal Activity Is Drastically Reduced in AC3 KO Mice

If there is neuronal atrophy associated with AC3 KO mice, then the synaptic or neuronal activity of AC3 KO mice will be reduced. Hence we monitored basal synaptic transmission at the CA3-CA1 synapse by electrically stimulating CA3-CA1 Schaffer-collateral synapses in the hippocampus. The field excitatory postsynaptic potential (fEPSP) was significantly lower in slices from AC3 KO mice compared to AC3 WT mice, while the amplitude of presynaptic volley was comparable (Fig 4A to 4C). Along with this, the population spikes in CA1 pyramidal layer were also examined. The amplitude of pop-spikes was consistently smaller in slices from AC3 KO mice than AC3 WT mice (Figure S1). Moreover, in whole cell recording of CA1 pyramidal neurons, both the amplitude and frequency of spontaneous EPSCs were strongly reduced in neurons from AC3 KO mice (Fig 4D to 4F). These data indicate that the normal synaptic function in CA3-CA1 synapses is significantly reduced in AC3 KO mice compared to AC3 WT mice. Interestingly, the resting membrane potentials of CA1 pyramidal neurons were more hyperpolarized in AC3 KO mice than AC3 WT mice (Fig 4G).

Synaptic activity governs neuronal activation. To test if CA1 neurons of AC3 KO mice are less active *in vivo* than AC3 WT mice in response to stimulation, we used fiber-optic fluorescence confocal endomicroscopy (FFE) to perform deep-brain calcium imaging [22, 23]. We first virally expressed a genetically encoded calcium indicator, GCaMP3 into the CA1 region of AC3 WT and AC3 KO mice. GCaMP3 expression in CA1 neurons was confirmed by immunostaining (Fig 4H). We then inserted a fiber fluorescence endomicroscope through a cannula to reach CA1 regions. FFE monitored the level of intracellular calcium in the cell body of GCaMP3-expressing neurons of free-behaving mice (Fig 4I). Upon electrical shock stimulation, a significant portion of CA1 neurons of AC3 WT mice displayed pronounced calcium spikes, while neurons of AC3 KO mice only

showed weak responses (Fig 4J–K). These data confirm that CA1 neurons of AC3 KO mice are less active than those of WT mice.

### AC3 KO Mice Exhibit Impaired Spatial Navigation and Depressed Long-Lasting LTP at the Schaffer-collateral Synapses

Depressed patients exhibit hippocampal structural abnormalities [27, 28] and the hippocampus is thought to play a major role in the pathology of MDD [29, 30]. Furthermore, depression is associated with cognition and memory impairments including defects in spatial navigation measured by whole-head magnetoencephalography coupled with navigation through a virtual Morris water maze [31]. Therefore, the spatial navigation of AC3 KO mice was evaluated using the Morris water maze, a hippocampus-dependent form of learning and memory. AC3 KO mice did not learn the location of the hidden platform in the Morris water task as readily as AC3 WT mice (Fig 5A), although their swim speeds were comparable ( $18 \pm 1$  cm/s for AC3 WT mice and  $17 \pm 2$  cm/s for AC3 KO mice,  $p=0.73$  by t-test). Moreover, in the probe test, AC3 KO mice did not show strong preferences for the original platform quadrant used in training (Fig 5B inset) and spent less time in the target quadrant than AC3 WT littermates (Fig 5C). The number of target-site crossing was also much lower in AC3 KO mice compared to AC3 WT mice (Fig 5C). These data indicate that like MDD patients, AC3 KO mice exhibit impaired spatial navigation.

We also examined AC3 KO mice for synaptic plasticity at the Schaffer-collateral synapse in the hippocampus. AC3 KO mice exhibited detrimental long-term potentiation (D-LTP), induced with one train of tetanus stimulation, comparable to AC3 WT mice (Fig 5D). However, long-lasting LTP (L-LTP), which was induced with 4 trains of tetanus, was significantly lower in AC3 KO mice and but it did persist for at least 150 min (Fig 5E). This suppression in hippocampal L-LTP is consistent with poorer spatial memory exhibited by AC3 KO mice and suggests that they may have deficits in synaptic plasticity.

In summary, AC3 KO mice exhibit characteristics largely mimicking the endophenotype of human depression (summarized in Table 1), supporting *ADCY3* as a candidate gene for MDD.

### Generation of AC3 Floxed Mice

However, AC3 is also expressed in other tissues such as olfactory sensory neurons [16] and the kidney [32]. To overcome the limitation of AC3 conventional KO mice and confirm the association of AC3 with depression, we have generated mice with conditional floxed *Adcy3* alleles. The recombinant targeting vector was designed so that exon 3 of the *Adcy3* gene was flanked by two loxP sites; 75 bp upstream and 75 bp downstream of exon 3. The exon 3 of *Adcy3* gene encodes part of the C1 enzymatic domain and knocking it out causes a frame shift and a premature stop codon (Fig. S2A). The targeting construct was confirmed by restriction assay (Fig. S2B). The insertion of neomycin gene distinguished the targeted allele (10.1kb) from wild type allele (8.6 kb) by 1.5kb (Fig. S2C). The critical region of the construct and the exon 2–6 of *Adcy3* was sequenced (100% collect, Fig. S3). Southern blot using 3' probe and neo probe screened over about 96 clones and obtained some positive ES clones (clone # 44, Fig. S2D and S2E). The ES cells of clone 44 were used for blastocyst



injection to develop chimeric mice. Mice with targeted allele were then crossed with the FLPER strain to delete the neo gene. PCR genotyping method was then used to select homologous AC3 floxed alleles (Fig. S2F).

### AC3 Forebrain KO mice Exhibit a Pro-depression Phenotype

Although depression involves in an overall reduction of brain activity, some parts of the brain are more affected than others. The prefrontal cortex, lateral habenula and hippocampus are critical regions strongly associated in mood disorders [3–5, 33], all located in the forebrain. Hence we aimed to ablate AC3 selectively in the forebrain. We selected an established forebrain-specific, *Emx1* promoter-driven Cre strain: *Emx1-Cre* mice [34], which expresses Cre recombinase specifically in the excitatory neurons in the forebrain [34]. The AC3 floxed mice were crossed with the *Emx1-Cre* mice for specific disruption of AC3 expression in the forebrain. Ablation of AC3 in excitatory neurons in the hippocampus and cortex in *AC3<sup>fr/fr</sup>; Emx1-Cre<sup>+</sup>* mice (“AC3 forebrain KO mice”), but not in control mice, was confirmed by immunostaining (Fig. 6A and Fig. S4–S5). AC3 forebrain KOs have normal size as controls (Fig. 6A). *Emx1-Cre* mouse strain does not express Cre in the main olfactory epithelia, which was verified through crossing it with a Td-Tomato Cre-reporter strain (Fig. S6). Hence, AC3 was unaffected in the olfactory epithelia and that the olfaction of AC3 forebrain KO mice would not be altered.

We examined if AC3 forebrain KO mice have depression-like behaviors. In the tail-suspension test, AC3 forebrain KO mice demonstrated markedly longer periods of immobility than controls (Fig. 6B). Similarly, AC3 forebrain KO mice exhibited longer periods of immobility in the forced swim test than controls (Fig. 6C). When feeding in a novel environment, AC3 forebrain KO mice were also much slower to feed than controls (Fig. 6D). Moreover, AC3 forebrain KO mice were less active than controls in their home cages during the night time (Fig. 6E). Consistently, AC3 forebrain KO mice were less active and moved a shorter distance than controls in the open field test (Fig. 6F). Nevertheless, AC3 forebrain KO mice did not show reduced sociability, spending similar time interacting with the target mouse relative to controls in a 3-chamber sociability test (Fig. 6G). AC3 forebrain KO mice spent a similar period of time in the open arm compared to controls (Fig. 6H), suggesting that they were not more anxious than control mice. However, AC3 forebrain KO mice had deficits in recognition memory and spatial navigation. In the novel object recognition test, AC3 forebrain KO mice did not recognize familiar object as well as controls (Fig. 6I). In the Morris water maze test, AC3 forebrain KO mice spent more time than controls in learning to identify the location of hidden platform (Fig. 6J). AC3 forebrain KO mice did not recognize the previous location of hidden platform as well as control mice in the probe test (Fig. 6K). Taken together, AC3 forebrain KO mice exhibited a pro-depression phenotype.

### AC3 Inducible KO Mice Exhibit a Pro-depression Phenotype

AC3 forebrain KO mice may contain subtle developmental defects. To completely circumvent developmental complications, we chose to inactivate AC3 temporally in adult mice. We have bred the AC3 floxed mice with a tamoxifen-inducible Cre mouse strain: “*Ubc-Cre/ERT2*”[35] to generate AC3 inducible KO mice. The Cre expression in *Ubc-Cre/*

ERT2 strain is driven by *Ubiquitin C* promoter and it has wide-spread Cre expression in the brain after administration of tamoxifen. Oral administration of tamoxifen to the AC3<sup>fl/fl</sup>:Ubc-Cre mice strongly removed AC3 expression in adult mice throughout the brain including the hippocampal CA1 region and cortex (Fig. S7). Henceforth we referred to the tamoxifen-induced AC3 knockout mice as “AC3 inducible KO mice”. There was another advantage for choosing Ubc-Cre/ERT2 mouse strain: after tamoxifen administration to the AC3 inducible KO mice to induce Cre expression, we observed that the electro-olfactogram responses in the main olfactory epithelia of the tamoxifen-inducible AC3 knockout mice were normal compared to controls and their ability to detect odorants remained intact (Fig. 7A and 7B). It rules out the possibility that the phenotype of inducible KOs was caused by an olfaction deficit.

AC3 inducible KO and WT mice were subjected to a set of depression-related behavioral tests. In the tail-suspension test, AC3 inducible KO mice demonstrated significantly longer periods of immobility than their littermate controls (Fig. 7C). Similarly, AC3 inducible KO mice exhibited longer periods of immobility in the forced swim test than WT mice (Fig. 7D). AC3 inducible KO mice had slightly longer latency to feed than controls in the novelty-suppressed feeding test (Fig. 7E). Moreover, the coat state of AC3 inducible KO mice was poor, which yielded a lower coat score compared to their WT mice (Fig. 7F), suggesting reduced grooming activity. AC3 inducible KO mice also performed poorly in building their nest compared to controls (Fig. 7G). Consistently, AC3 inducible KO mice were also less active than controls in their home cages during night time (Fig. 7H and Fig. S8). To test if AC3 inducible KO mice have sleep problems, we performed EEG/EMG recording and sleep analysis. Indeed, AC3 inducible KO mice demonstrated altered sleep architecture compared to controls. The sleep-wake cycle was not very rhythmic in AC3 inducible KO mice compared to controls (Fig. 7I) and had more NREM sleep in night-time and less NREM sleep in day-time than controls (Fig. 7J–K). These data indicate that AC3 inducible KO mice have an altered sleep pattern, in line with depression-like behaviors. Collectively, these data support that AC3 inducible KO mice demonstrate depression-like phenotypes.

## DISCUSSION

MDD is a complex, heterogeneous mental disorder characterized by depressive episodes and loss of interest or pleasure in normally enjoyable activity [36]. Depressed patients exhibit a number of disturbances including cognitive defects [37], smaller brain size [38, 39], altered sleep pattern [26], and deficits in spatial navigation [31]. Although environmental factors including stress [14] may contribute to depression, MDD is familial and both onset and recurrence of depression are associated with higher familial aggregation [40, 41]. A genome-wide association study of the MDD patients identified adenylyl cyclase 3 (*ADCY3*, 2p23.3) as a top ranked gene for MDD [14]. The objective of this study was to explore if disruption of AC3 in the brain leads to depression-related phenotypes in mice.

Using a battery of behavioral assays for depression including the tail suspension test, forced swim test, novelty-suppressed feeding and nesting behavior test, we found that AC3 KO mice exhibit depression-like behaviors. Like MDD patients [25, 26], the sleep architecture of AC3 KO mice is perturbed with higher levels of REM sleep and altered NREM sleep. AC3



KO mice have smaller hippocampi than wild-type mice and demonstrate deficits in hippocampus-dependent spatial navigation and L-LTP in the hippocampus. Collectively, AC3 KO mice exhibit many behavioral and physical phenotypes associated with MDD (Table 1), thereby providing evidence for the hypothesis that the *ADCY3* gene may play a role in depression. Furthermore, we generated a strain of *Adcy3* floxed mice, which allowed us to inactivate AC3 in a temporal or tissue-specific manner. We first prepared the AC3 forebrain KO mice, which demonstrated pro-depression phenotypes as well as memory deficit. Consistently, AC3 inducible KO mice, which completely avoided the developmental complications, also exhibited pro-depression phenotypes including impaired nesting behaviors, reduced coat score and altered sleep architecture. All together, these data strongly support the hypothesis that AC3 is a contributing factor for depression.

Why does loss of AC3 lead to depression? It is likely caused by reduced neuronal activity in the CNS. A notable property of AC3 KO mice is that basal synaptic activity including field excitatory postsynaptic potential and spontaneous EPSCs are significantly depressed (Fig 4). Moreover, calcium imaging *in vivo* provides evidence that hippocampal CA1 neurons had reduced activation in response to foot shock (Fig 4). This general decrease in neuronal activity may contribute to the depressed behavior of AC3 KO mice and may be due to the fact that AC3 is expressed almost exclusively in primary cilia of CNS neurons [11, 12]. Primary cilia are the sensory antenna in most mammalian cells and are unique and sensitive signaling compartment [42]. Cyclic AMP generated by AC3 in primary cilia regulates arborization of dendrites and thereby can affect synaptic activity in the hippocampus and other areas of the brain [18]. This is consistent with reports suggesting that primary cilia may play a regulatory role in dendritic refinement and synaptic integration of adult-born neurons [43]. This study provides evidence, suggesting that AC3 in primary cilia regulates neuronal morphology and neuronal activity, deficits of which may lead to depression-like phenotypes.

One might argue that the anosmia of AC3 KO mice [16] may cause depression since depression may be due to interactions between genetic susceptibility and environmental factors. Loss of smell severely interferes with the interaction of mice with conspecific and environments, which could lead to some defects in mouse behaviors. Nevertheless, it has been shown that anosmia caused by ablation of the gene for cyclic nucleotide gated ion channels (CNG) in the main olfactory epithelium does not lead to depression in mice [44]. Importantly, both AC3 forebrain KO mice and AC3 inducible KO mice exhibited pro-depression phenotype but both strains retain olfactory perception. Thus, anosmia may partly contribute to but is unlikely to be the major cause of the depressive phenotypes.

The data reported in this study and in the genome-wide association study of the MDD patients [14] support the possibility that AC3 is a contributing factor for major depression. This study also implies a novel strategy to combat depression by targeting the cAMP signaling specifically in neuronal cilia. Nevertheless, further work is warranted to establish the role of ciliary cAMP signaling in major depression and reveal its molecular mechanism.

## Supplementary Material

Refer to Web version on PubMed Central for supplementary material.

## Acknowledgments

This study was supported by NIH grants DC004156 and MH073601 to D.R.S., MH105746 to X.C., and MH098177 to L.S.Z. and by the Howard Hughes Medical Institute to R.D.P.

## References

1. Lecrubier Y. The burden of depression and anxiety in general medicine. *J Clin Psychiatry*. 2001; 62(Suppl 8):4–9. discussion 10–11.
2. Wong ML, Licinio J. From monoamines to genomic targets: a paradigm shift for drug discovery in depression. *Nat Rev Drug Discov*. 2004; 3:136–151. [PubMed: 15040578]
3. Drevets WC, Price JL, Simpson JR Jr, Todd RD, Reich T, Vannier M, Raichle ME. Subgenual prefrontal cortex abnormalities in mood disorders. *Nature*. 1997; 386:824–827. [PubMed: 9126739]
4. Duman RS, Aghajanian GK. Synaptic dysfunction in depression: potential therapeutic targets. *Science*. 2012; 338:68–72. [PubMed: 23042884]
5. Eisch AJ, Petrik D. Depression and hippocampal neurogenesis: a road to remission? *Science*. 2012; 338:72–75. [PubMed: 23042885]
6. Sapolsky RM. Depression, antidepressants, and the shrinking hippocampus. *Proc Natl Acad Sci U S A*. 2001; 98:12320–12322. [PubMed: 11675480]
7. Tabakoff B, Hoffman PL. Transducing emotionality: the role of adenylyl cyclases. *Biol Psychiatry*. 2012; 71:572–573. [PubMed: 22424112]
8. Menninger JA, Tabakoff B. Forskolin-stimulated platelet adenylyl cyclase activity is lower in persons with major depression. *Biol Psychiatry*. 1997; 42:30–38. [PubMed: 9193739]
9. Hines LM, Tabakoff B. State, W.I.S.o., Trait Markers of Alcohol, U., and Dependence, I. Platelet adenylyl cyclase activity: a biological marker for major depression and recent drug use. *Biol Psychiatry*. 2005; 58:955–962. [PubMed: 16095566]
10. Katsel PL, Tagliente TM, Schwarz TE, Craddock-Royal BD, Patel ND, Maayani S. Molecular and biochemical evidence for the presence of type III adenylyl cyclase in human platelets. *Platelets*. 2003; 14:21–33. [PubMed: 12623444]
11. Bishop GA, Berbari NF, Lewis J, Mykytyn K. Type III adenylyl cyclase localizes to primary cilia throughout the adult mouse brain. *The Journal of comparative neurology*. 2007; 505:562–571. [PubMed: 17924533]
12. Wang Z, Li V, Chan GC, Phan T, Nudelman AS, Xia Z, Storm DR. Adult type 3 adenylyl cyclase-deficient mice are obese. *PloS one*. 2009; 4:e6979. [PubMed: 19750222]
13. Atlantis E, Sullivan T. Bidirectional association between depression and sexual dysfunction: a systematic review and meta-analysis. *J Sex Med*. 2012; 9:1497–1507. [PubMed: 22462756]
14. Wray NR, Pergadia ML, Blackwood DH, Penninx BW, Gordon SD, Nyholt DR, Ripke S, MacIntyre DJ, McGhee KA, Maclean AW, et al. Genome-wide association study of major depressive disorder: new results, meta-analysis, and lessons learned. *Mol Psychiatry*. 2012; 17:36–48. [PubMed: 21042317]
15. Redei EE, Andrus BM, Kwasny MJ, Seok J, Cai X, Ho J, Mohr DC. Blood transcriptomic biomarkers in adult primary care patients with major depressive disorder undergoing cognitive behavioral therapy. *Transl Psychiatry*. 2014; 4:e442. [PubMed: 25226551]
16. Wong ST, Trinh K, Hacker B, Chan GC, Lowe G, Gaggari A, Xia Z, Gold GH, Storm DR. Disruption of the type III adenylyl cyclase gene leads to peripheral and behavioral anosmia in transgenic mice. *Neuron*. 2000; 27:487–497. [PubMed: 11055432]
17. Chen X, Xia Z, Storm DR. Stimulation of electro-olfactogram responses in the main olfactory epithelia by airflow depends on the type 3 adenylyl cyclase. *The Journal of neuroscience: the official journal of the Society for Neuroscience*. 2012; 32:15769–15778. [PubMed: 23136416]

18. Guadiana SM, Semple-Rowland S, Daroszewski D, Madorsky I, Breunig JJ, Mykytyn K, Sarkisian MR. Arborization of dendrites by developing neocortical neurons is dependent on primary cilia and type 3 adenylyl cyclase. *The Journal of neuroscience: the official journal of the Society for Neuroscience*. 2013; 33:2626–2638. [PubMed: 23392690]
19. Chen X, Qiu L, Li M, Durnagel S, Orser BA, Xiong ZG, MacDonald JF. Diarylamidines: high potency inhibitors of acid-sensing ion channels. *Neuropharmacology*. 2010; 58:1045–1053. [PubMed: 20114056]
20. Chen X, Whissell P, Orser BA, MacDonald JF. Functional modifications of acid-sensing ion channels by ligand-gated chloride channels. *PloS one*. 2011; 6:e21970. [PubMed: 21789198]
21. Blanton MG, Lo Turco JJ, Kriegstein AR. Whole cell recording from neurons in slices of reptilian and mammalian cerebral cortex. *Journal of neuroscience methods*. 1989; 30:203–210. [PubMed: 2607782]
22. Chen X, Cao H, Saraf A, Zweifel LS, Storm DR. Overexpression of the type 1 adenylyl cyclase in the forebrain leads to deficits of behavioral inhibition. *The Journal of neuroscience: the official journal of the Society for Neuroscience*. 2015; 35:339–351. [PubMed: 25568126]
23. Gore BB, Soden ME, Zweifel LS. Visualization of plasticity in fear-evoked calcium signals in midbrain dopamine neurons. *Learning & memory*. 2014; 21:575–579. [PubMed: 25320348]
24. Soden ME, Jones GL, Sanford CA, Chung AS, Gueler AD, Chavkin C, Lujan R, Zweifel LA. Disruption of Dopamine Neuron Activity Pattern Regulation through Selective Expression of a Human KCNN3 Mutation. *Neuron*. 2013 in press.
25. Pillai V, Kalmbach DA, Ciesla JA. A meta-analysis of electroencephalographic sleep in depression: evidence for genetic biomarkers. *Biol Psychiatry*. 2011; 70:912–919. [PubMed: 21937023]
26. Palagini L, Baglioni C, Ciapparelli A, Gemignani A, Riemann D. REM sleep dysregulation in depression: state of the art. *Sleep Med Rev*. 2013; 17:377–390. [PubMed: 23391633]
27. Campbell S, Marriott M, Nahmias C, MacQueen GM. Lower hippocampal volume in patients suffering from depression: a meta-analysis. *The American journal of psychiatry*. 2004; 161:598–607. [PubMed: 15056502]
28. Videbech P, Ravnkilde B. Hippocampal volume and depression: a meta-analysis of MRI studies. *The American journal of psychiatry*. 2004; 161:1957–1966. [PubMed: 15514393]
29. Sahay A, Hen R. Adult hippocampal neurogenesis in depression. *Nature neuroscience*. 2007; 10:1110–1115. [PubMed: 17726477]
30. Perera TD, Park S, Nemirovskaya Y. Cognitive role of neurogenesis in depression and antidepressant treatment. *The Neuroscientist: a review journal bringing neurobiology, neurology and psychiatry*. 2008; 14:326–338.
31. Cornwell BR, Salvatore G, Colon-Rosario V, Latov DR, Holroyd T, Carver FW, Coppola R, Manji HK, Zarate CA Jr, Grillon C. Abnormal hippocampal functioning and impaired spatial navigation in depressed individuals: evidence from whole-head magnetoencephalography. *The American journal of psychiatry*. 2010; 167:836–844. [PubMed: 20439387]
32. Pluznick JL, Zou DJ, Zhang X, Yan Q, Rodriguez-Gil DJ, Eisner C, Wells E, Greer CA, Wang T, Firestein S, et al. Functional expression of the olfactory signaling system in the kidney. *Proc Natl Acad Sci U S A*. 2009; 106:2059–2064. [PubMed: 19174512]
33. Li K, Zhou T, Liao L, Yang Z, Wong C, Henn F, Malinow R, Yates JR 3rd, Hu H. betaCaMKII in lateral habenula mediates core symptoms of depression. *Science*. 2013; 341:1016–1020. [PubMed: 23990563]
34. Gorski JA, Talley T, Qiu M, Puelles L, Rubenstein JL, Jones KR. Cortical excitatory neurons and glia, but not GABAergic neurons, are produced in the Emx1-expressing lineage. *The Journal of neuroscience: the official journal of the Society for Neuroscience*. 2002; 22:6309–6314. [PubMed: 12151506]
35. Ruzankina Y, Pinzon-Guzman C, Asare A, Ong T, Pontano L, Cotsarelis G, Zediak VP, Velez M, Bhandoola A, Brown EJ. Deletion of the developmentally essential gene ATR in adult mice leads to age-related phenotypes and stem cell loss. *Cell Stem Cell*. 2007; 1:113–126. [PubMed: 18371340]
36. Nelson JC, Charney DS. The symptoms of major depressive illness. *The American journal of psychiatry*. 1981; 138:1–13. [PubMed: 7446757]

37. Murrough JW, Iacoviello B, Neumeister A, Charney DS, Iosifescu DV. Cognitive dysfunction in depression: neurocircuitry and new therapeutic strategies. *Neurobiology of learning and memory*. 2011; 96:553–563. [PubMed: 21704176]
38. Arnone D, McKie S, Elliott R, Juhasz G, Thomas EJ, Downey D, Williams S, Deakin JF, Anderson IM. State-dependent changes in hippocampal grey matter in depression. *Mol Psychiatry*. 2013; 18:1265–1272. [PubMed: 23128153]
39. Koolschijn PC, van Haren NE, Lensvelt-Mulders GJ, Hulshoff Pol HE, Kahn RS. Brain volume abnormalities in major depressive disorder: a meta-analysis of magnetic resonance imaging studies. *Hum Brain Mapp*. 2009; 30:3719–3735. [PubMed: 19441021]
40. Sullivan PF, Neale MC, Kendler KS. Genetic epidemiology of major depression: review and meta-analysis. *The American journal of psychiatry*. 2000; 157:1552–1562. [PubMed: 11007705]
41. Kendler KS, Gatz M, Gardner CO, Pedersen NL. Age at onset and familial risk for major depression in a Swedish national twin sample. *Psychol Med*. 2005; 35:1573–1579. [PubMed: 16219115]
42. Singla V, Reiter JF. The primary cilium as the cell's antenna: signaling at a sensory organelle. *Science*. 2006; 313:629–633. [PubMed: 16888132]
43. Kumamoto N, Gu Y, Wang J, Janoschka S, Takemaru K, Levine J, Ge S. A role for primary cilia in glutamatergic synaptic integration of adult-born neurons. *Nature neuroscience*. 2012; 15:399–405. S391. [PubMed: 22306608]
44. Glinka ME, Samuels BA, Diodato A, Teillon J, Feng Mei D, Shykind BM, Hen R, Fleischmann A. Olfactory deficits cause anxiety-like behaviors in mice. *The Journal of neuroscience: the official journal of the Society for Neuroscience*. 2012; 32:6718–6725. [PubMed: 22573694]
45. Wang Z, Balet Sindreu C, Li V, Nudelman A, Chan GC, Storm DR. Pheromone detection in male mice depends on signaling through the type 3 adenylyl cyclase in the main olfactory epithelium. *The Journal of neuroscience: the official journal of the Society for Neuroscience*. 2006; 26:7375–7379. [PubMed: 16837584]

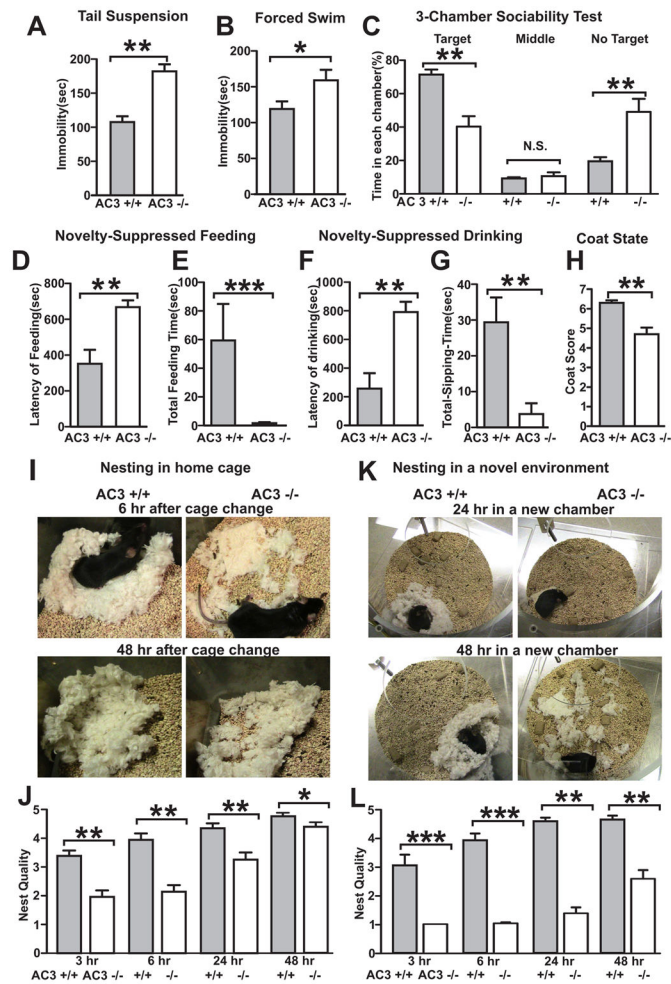


**Fig. 1.** AC3 KO mice ( $AC3^{-/-}$ ) exhibit depression-like behaviors. (A) Tail suspension test. The time that AC3 KO mice were immobile was significantly greater than AC3 WT littermates ( $AC3^{+/+}$ ). (B) Forced swim test. AC3 KO mice were immobile for greater periods of time than AC3 WT mice during the forced swim test. (C) 3-chamber sociability test. AC3 KO mice spend less time in the chamber with interacting target and more time in chamber without target than AC3 WT mice. (D and E) Novelty-suppressed feeding test. The latency to feed in a novel environment was greater in AC3 KO mice than AC3 WT mice (D). The total feeding time for AC3 KO mice was significantly less than AC3 WT mice (E). (F and G) Novelty-suppressed drinking test. The latency of drinking was greater in AC3 KO mice than AC3 WT mice (F). The total feeding time of AC3 KO mice was significantly less than AC3 WT mice (G). (H) The coat score of AC3 KO mice was lower than WT mice. (I–L) Nesting behavior in home cage (I and J) and in a novel environment (K and L). Representative photos of nests were shown (I and K) and scores of nest at 4 different time points were analyzed (J and L). AC3 KO mice were slow in building nest and made bad nest compared to AC3 WT mice in home cages (J). The nesting behavior of AC3 KO mice was exacerbated in a novel environment (L). For all tests,  $n = 7-14$ ; \*  $p < 0.05$ ; \*\*  $p < 0.01$ .

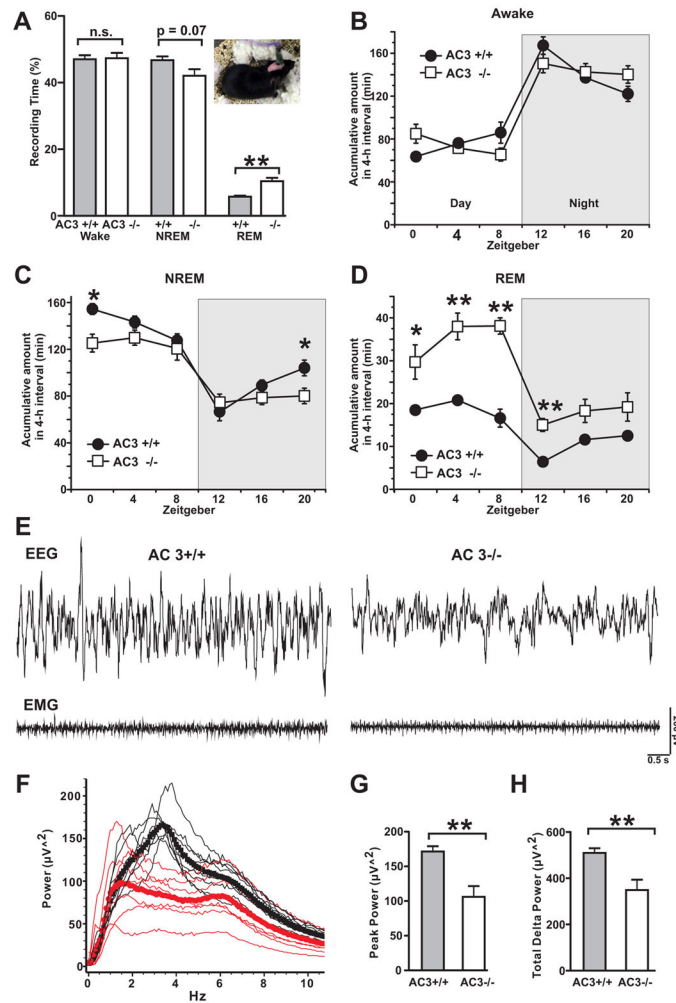


**Fig. 2.** AC3 KO mice exhibit increased amounts of REM sleep and have altered NREM sleep. (A) Percentage time spent awake, in NREM sleep and REM sleep in 24 hours. Inset is a mouse picture during EEG/EMG recording. (B) Time spent awake (accumulated time in 4-h intervals). (C) Time spent in NREM sleep (accumulated time in 4-h intervals). (D) Time spent in REM sleep (accumulated time in 4-h intervals). Nighttime is indicated by a shaded background. ZT0, onset of the light phase; ZT12, onset of dark phase. (E) Representative EEG and EMG sweeps of NREM sleep of AC3 WT and KO mice. (F) Power analysis (in 0.1 Hz bin) of NREM sleep over 24-h. Thin lines are power spectrum from individual mice. Black is for AC3 WT and red for AC3 KO mice. Squares (AC3 WT, black) and circles (AC3 KO, red) are averaged power spectrum from 8–9 mice. (G) Peak power (power at peak frequency) of NREM sleep of AC3 WT and AC3 KO mice. (H) Total delta power (summed power from 0–4.5 Hz frequency, 0.1 Hz bin) of NREM sleep.  $n = 8-9$ ; \*\* $p < 0.01$ .



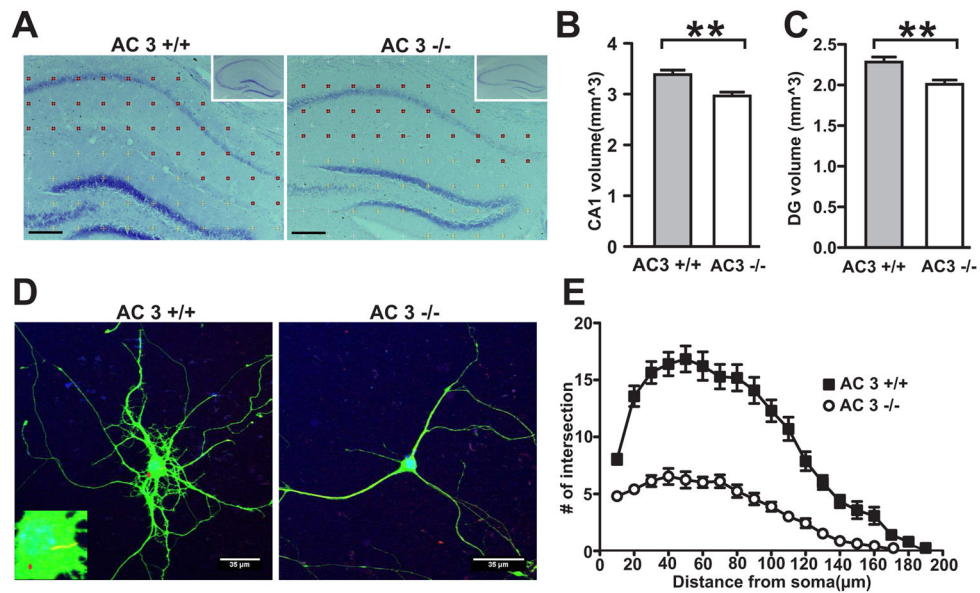


**Fig. 3.** AC3 KO mice demonstrate neuronal atrophy. (A–C) AC3 KO mice have smaller hippocampal volume. The Nissl-stained hippocampus at the comparable location from AC3 WT and AC3 KO mice (A) with a 150- $\mu$ m grid overlay used for Cavalieri volume estimations. Insets show representative whole hippocampal images with a lower magnification. Scale bar, 200  $\mu$ m. CA1, closed circles; DG (dentate gyrus), open circles. (B) CA1 volume is smaller in AC3 KO mice than that of AC3 WT mice. (C) The volume of dentate gyrus is smaller than in mice.  $n = 6$  pairs; \*\*,  $p < 0.01$ . (D–E) Primarily cultured cortical neurons from AC3 KO mice have fewer dendritic arborization. (D) Representative image of cortical neurons at 12 days *in vitro* from AC3 WT and AC3 KO mice. Green: anti-GFP staining. Red arrow indicates the stained AC3 in the primary cilium (left, inset), which was absent in AC3 KO mice (right). (E) Sholl analyses revealed the extent of arborization of cultured cortical neurons. Two-way ANOVA,  $F(1, 1500) = 462$ ,  $p < 0.0001$ . Cultured neurons were from 5 AC3 WT mice and 4 AC3 KO mice.

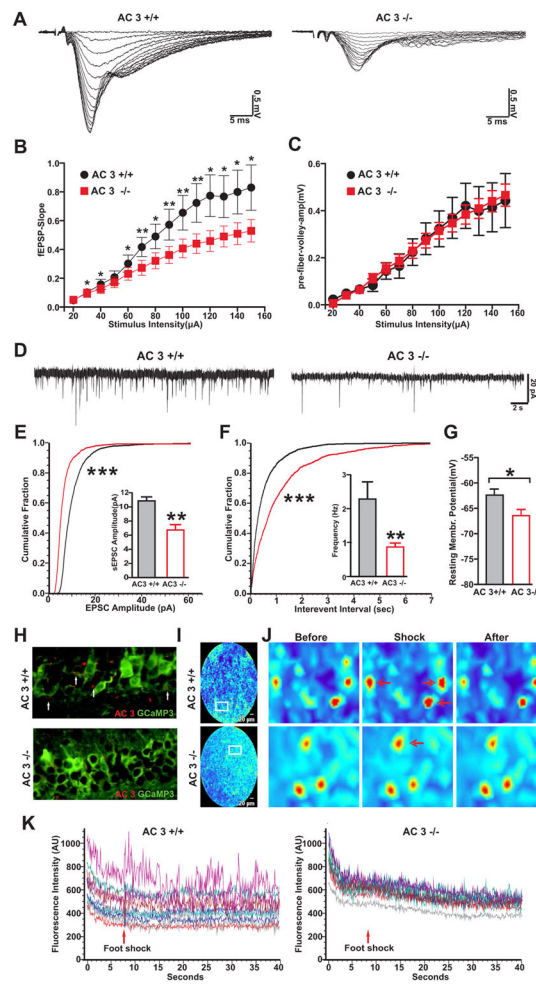


**Fig. 4.** CA3-CA1 synaptic activity is reduced in hippocampal slices from AC3 KO mice. (A–C) Evoked electrical responses in CA3-CA1 synapses of AC3 KO mice were markedly smaller than those from AC3 WT mice. Synaptic responses were electrically elicited with varying stimulation intensity (0–150  $\mu$ A). (A) Representative synaptic responses (super-imposed) of AC3 WT (left) and KO (right) mice. (B) Slope of field EPSP plotted against stimulus intensity. (C) Field EPSP slope plotted against the amplitude of presynaptic volley.  $n = 16$  for AC3 WTs and  $n = 19$  for AC3 KO mice \* $p < 0.05$ ; \*\* $p < 0.01$ . (D–F) Spontaneous excitatory postsynaptic current (sEPSC) recorded from CA1 pyramidal neurons in whole cell patch-clamp recordings. (D) Representative sEPSC recorded from CA1 pyramidal layer; right, AC3 WT; left, AC3 KO. (E and F) Cumulative plot and average values (insets) of sEPSC amplitude (E) and frequency (F).  $n = 7$  for AC3 WT and  $n = 9$  for AC3 KO. \*\*\* $p < 0.001$  by Kolmogorov-Smirnov test, \*\* $p < 0.01$  by t-test. (G) The resting membrane potential of CA1 pyramidal neuron of AC3 KO mice was more hyperpolarized than that of AC3 WT mice.  $n = 8$  per genotype, \* $p < 0.05$ . (H–K) CA1 neurons from AC3 KO mice are less responsive to foot shock stimulation. (H) AC3 WT and AC3 KO mice were injected with AAV1 expressing a calcium indicator GCaMP3 into CA1 region. Representative image of CA1 neurons stained with anti-GFP (green, recognizing the GCaMP3) and anti-AC3

antibodies. Primary cilia marker of AC3 (arrows) was present in AC3 WT mice but absent in AC3 KO mice. (I) Representative full-field images of CA1 region in free-running mice using FFE. (J) 3 panels: zoom-in representative images before, during and after foot shock. Some neurons responded to foot shock (red arrows). (K) Time course of fluorescence intensity of 12 randomly selected cells by FFE calcium imaging. Foot shock induced calcium spikes (changed fluorescence intensity). The increase in the fluorescence in response to foot shock was much smaller in AC3 KO mice (right) compared to WT mice (left). n = 4 pairs of mice. 12–24 neurons from each mouse were analyzed.

Author Manuscript

Author Manuscript

Author Manuscript

Author Manuscript

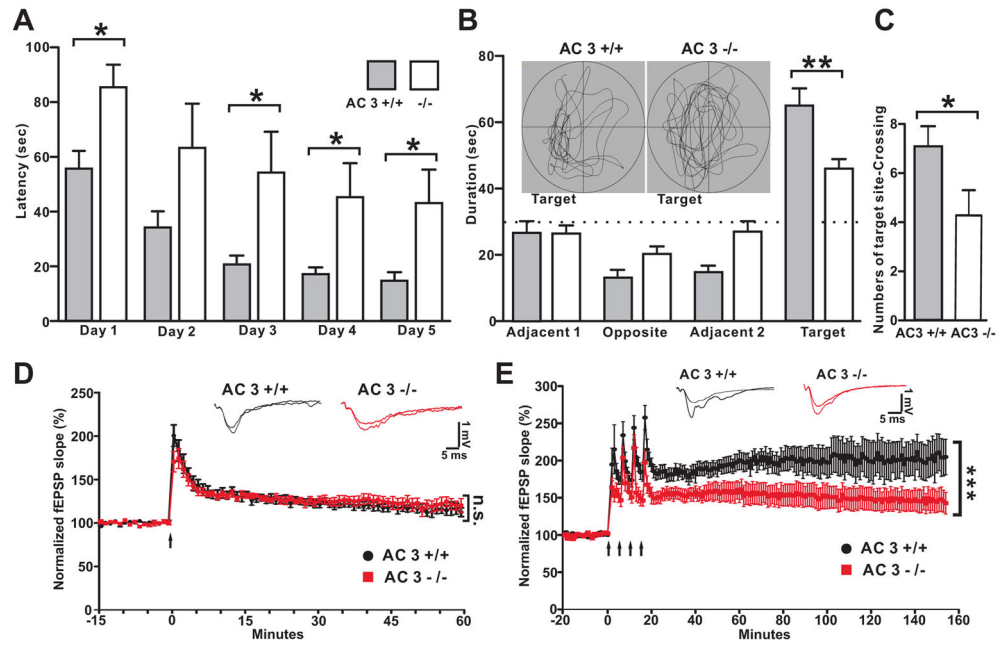


**Fig. 5.**

AC3 KO mice exhibit deficits in spatial navigation and suppressed Long-lasting LTP (L-LTP). (A) Learning curve for the hidden platform test in the Morris water maze. Data are averages of 3 trials each day. (B) Time in each quadrant during the probe test. Inset: representative swimming pattern during the probe test. (C) Number of target site crossings during the probe test. (D–E) Suppressed L-LTP in mice. Decremental LTP (D-LTP) was induced with one train of tetanus stimulation (D), while L-LTP was induced by 4 trains of tetanus stimulation (E). Top insets: representative field EPSPs before and at 60 min (D-LTP) or at 150 min (L-LTP) after LTP induction. D-LTP of AC3 KO mice was comparable to AC3 WT mice, (Two-way ANOVA test comparing data points of last 10 min, genotype effect,  $F(1, 117) = 0.53, p=0.48$ ), while L-LTP was attenuated in AC3 KO mice (Two-way ANOVA test comparing data of last 20 min, genotype effect,  $F(1, 216) = 101, p<0.0001$ ).

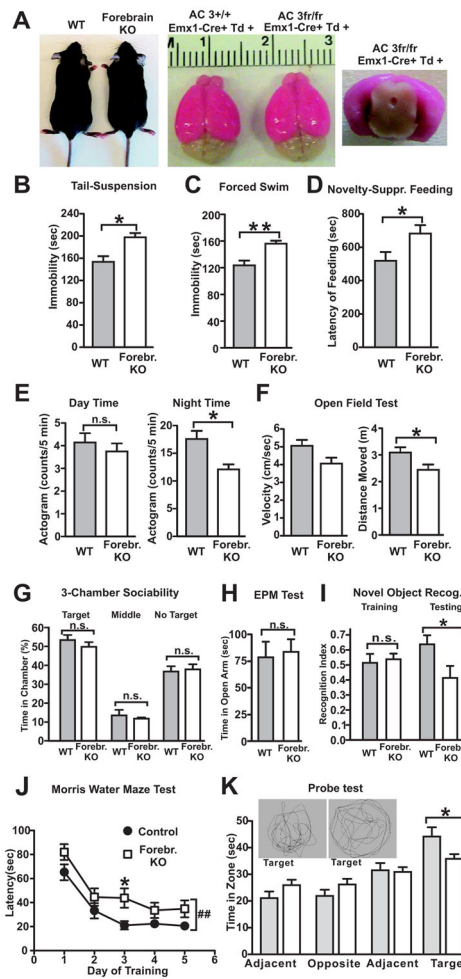


**Fig. 6.** AC3 forebrain KO mice exhibit pro-depression behaviors. From A–K, WT (AC3 control mice): AC3<sup>+/+</sup>;Emx1-Cre<sup>+</sup>; Forebr. KO (AC3 Forebrain KO mice): AC3<sup>fr/fr</sup>; Emx1-Cre<sup>+</sup>. (A) AC3 Forebrain KOs have normal grow rate (left) and EMX1-promoter driven Cre recombinase was expressed specifically in the forebrain as monitored by a Td-Tomato Cre-reported stain (middle and right). (B) Tail-suspension test. The time that AC3 forebrain KO mice were immobile was significantly greater than controls. (C) Forced swim test. AC3 forebrain KO mice were immobile for longer periods of time than controls during the forced swim test. (D) Novelty-suppressed feeding test. The latency to feed in a novel environment was greater in AC3 forebrain KO mice than control mice. (E) Mouse activity during day and during the night. AC3 forebrain KO mice had more activity than control mice at night time. (F) Open field test. The distance moved by AC3 forebrain KO mice in an open field was longer than in control mice. (G) 3-chamber sociability test. AC3 forebrain KO mice and littermate controls mice spent comparable time in each chamber. (H) Elevated plus maze test. AC3 forebrain KO mice and littermate controls spent comparable time in the open arm in the elevated-plus maze test. (I–K) AC3 forebrain KO mice had reduced recognition and spatial memory. (I) Novel objection recognition test. AC3 forebrain KO mice and control mice spent similar time in exploring A1 and A2 during training, but AC3 forebrain KO mice

didn't recognize the familiar object as well as control mice during the test. (J–K) Morris water maze test. (J) Learning curve for the hidden platform test in the Morris water maze. Data are averages of 3 trials each day. AC3 forebrains KO mice were slower to identify the hidden platform than control mice. Two-way ANOVA with Bonferroni post tests, genotype effect,  $F(1, 92) = 9.99$ ,  $p = 0.004$ , data were from  $n = 12$  control mice and 13 AC3 forebrain KO mice. (K) Time in each quadrant during the probe test. Inset: representative swimming pattern during the probe test. For all tests except section J,  $n = 6–14$ ; n.s. not significant, \*  $p < 0.05$ ; \*\*  $p < 0.01$  by Student t test.



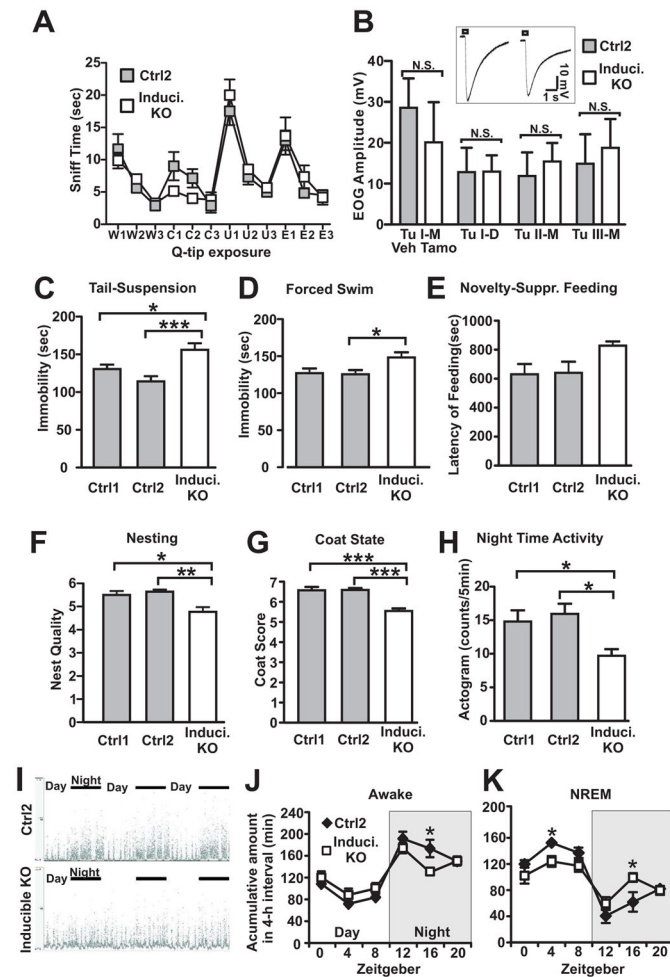


**Fig. 7.** AC3 inducible KO mice demonstrate depression-like phenotypes. From A–K, Ctrl1: AC3<sup>fr/fr</sup>: no-Cre, tamoxifen-treated mice; Ctrl2: AC3<sup>fr/fr</sup>:Ubc-Cre, vehicle-treated mice; Induci. KO: AC3<sup>fr/fr</sup>:Ubc-Cre, tamoxifen-treated mice. (A) AC3 inducible KO mice retained odor-sensing ability. Olfactory habituation/dishabituation test. w1, w2, and w3: the first, second, third water Q-tip exposure; three times of citralva (denote as C in Figure), three times male mouse urine (U), and three times eugenol (E). Q-tips were exposed subsequently. AC3 inducible KO mice and controls spent comparable time to sniff most of odorant Q-tips except that AC3 inducible KO mice sniffed shorter during the citralva exposure. Data were from 8 vehicle-treated control mice and 8 tamoxifen-treated inducible KO mice. (B) The electroolfactogram (EOG) responses in the main olfactory epithelia of AC3 inducible KO mice were similar to controls. Field potential amplitude of EOG responses at different sites in turbinates I, II, and III are shown. D, dorsal; M, middle. Inset shows representative traces of EOG recording (site: middle of turbinate II) from control mice and AC3 inducible KO mice. Data were from 6 vehicle-treated control mice and 7 tamoxifen-treated inducible KO mice. (C) Tail-suspension test. The time that AC3 inducible KO mice were immobile was significantly greater than controls. (D) Forced swim test. AC3 inducible KO mice were immobile for longer periods of time than controls during the forced swim test. (E) Novelty-

suppressed feeding test. The latency to feed in a novel environment was slightly longer in AC3 inducible KO mice than control mice. (F) Nesting behavior. The score of nest built by AC3 inducible KO mice was lower than that of their controls. (G) The coat score of AC3 inducible KO mice was lower than controls. (H) Mouse activity during day/night. AC3 inducible KO mice had more activity than control mice during night time. For experiments from section C–H:  $n = 7–13$ , \*  $p < 0.05$ ; \*\*  $p < 0.01$ ; \*\*\*  $p < 0.001$  by one way ANOVA with Tukey post hoc tests. (I–K) AC3 inducible KO mice had altered sleep architecture. (I) Representative normalized EMG power of neck muscle in 3 days/nights. Top, Control mice (AC3<sup>fl/fl</sup>:Ubc-Cre, vehicle-treated); bottom, AC3 inducible KO mice (AC3<sup>fl/fl</sup>:Ubc-Cre, tamoxifen-treated). (J–K) Accumulated time (in 4 hour intervals) spent awake (J) and NREM (K) were plotted against zeitgeber. Nighttime is indicated by a shaded background. ZT0, onset of the light phase; ZT12, onset of dark phase. \*  $p < 0.05$  by Student t-test. EEG/EMG data were from 6 vehicle-treated control mice and 8 tamoxifen-treated inducible KO mice.

**Table 1**

Comparison of Symptoms of MDD with Phenotypes of AC3 KO Mice

Symptoms of Human MDD (DSM-5)	Phenotypes of AC3 KO Mice
Despair	Reduced mobility in tail suspension and forced swim test
Psychomotor retardation/or agitation	Hypocomotor activities
Lack of motivation	Impaired nesting behavior
Eating disorder	Hyperphagia in home cage; Suppressed feeding in novel environments
Sleeping alteration; increased REM sleep	Increased REM sleep; shallow NREM sleep
Reduced sexual drive or sexual activities	Defects of sexual behaviors (Wang et al., 2011a)
Small cortex and hippocampi	Smaller brain, reduced volume of hippocampi
Memory deficit	Deficit in spatial navigation
Cognitive dysfunction	Defect in novel object recognition (Wang et al., 2011b)
Social withdraw or social isolation	Impaired sociability
Reduced smell sensitivity	Anosmia
Suicide attempt, feeling of guilty	No applicable

Author Manuscript

Author Manuscript

Author Manuscript

Author Manuscript